KAJIKAWA, Y., MUKAI, K., ISHIZU, K. & OJIMA, H. (1981). *Chem. Lett.* pp. 801–804.

KAJIKAWA, Y., SAKURAI, T., AZUMA, N., KOHNO, S., TSUBOYAMA, S., KOBAYASHI, K., MUKAI, K. & ISHIZU, K. (1984). *Bull. Chem. Soc. Jpn.* To be published.

MAIN, P., HULL, S. E., LESSINGER, L., GERMAIN, G., DECLERCQ, J.-P. & WOOLFSON, M. M. (1978). *MULTAN 78. A System of Computer Programs for the Automatic Solution of Crystal Structures from X-ray Diffraction Data.* Univs. of York, England, and Louvain, Belgium.

MULQI, F. S., STEPHENS, F. S. & VAGG, R. S. (1981). *Inorg. Chim. Acta*, **51**, 9–14.

NEWTON, N. D. (1983). *Acta Cryst.* B**39**, 104–113.

OJIMA, H. (1967). *Nippon Kagaku Zasshi*, **88**, 333–339.

SAKURAI, T. & KOBAYASHI, K. (1979). *Rikagaku Kenkyusho Hokoku*, **55**, 69–77.

SIGEL, H. & MARTIN, R. B. (1982). *Chem. Rev.* **82**, 385–426.

STEPHENS, F. S. & VAGG, R. S. (1981). *Inorg. Chim. Acta*, **51**, 149–154.

STEPHENS, F. S. & VAGG, R. S. (1982). *Inorg. Chim. Acta*, **57**, 43–49.

Acta Cryst. (1984). B**40**, 473–478

Crystalline-State Reaction of Cobaloxime Complexes by X-ray Exposure. VIII. Effect of the Cooperative Motion on the Reaction Rate

BY AKIRA UCHIDA, YUJI OHASHI* AND YOSHIO SASADA

Laboratory of Chemistry for Natural Products, Tokyo Institute of Technology, Nagatsuta 4259, *Midori-ku, Yokohama* 227, *Japan*

YOSHIAKI OHGO

Niigata College of Pharmacy, 5829 *Kamishinei-cho, Niigata* 950-21, *Japan*

AND SHOE BABA

Niigata Academy of Medical Technology, 5829 *Kamishinei-cho, Niigata* 950-21, *Japan*

(*Received* 28 *February* 1984; *accepted* 4 *May* 1984)

Abstract

Crystals of [(*R*)-1-cyanoethyl]bis(dimethylglyoximato)(4-methylpyridine)cobalt(III) (dimethylglyoximato = 2,3-butanedione dioximato), $C_{17}H_{25}CoN_6O_4$, $[Co(C_3H_4N)(C_6H_7N)(C_4H_7N_2O_2)_2]$, reveal crystalline-state racemization on exposure to X-rays. At the initial stage, the crystal is monoclinic, space group $P2_1$, with $a = 8{\cdot}875\ (7)$, $b = 28{\cdot}525\ (10)$, $c = 8{\cdot}695\ (5)$ Å, $\beta = 115{\cdot}59\ (6)°$, $V = 1985\ (2)$ Å^3, $M_r = 436{\cdot}4$, $D_m = 1{\cdot}47$, $D_x = 1{\cdot}508$ g cm^{-3} for $Z = 4$ and μ(Mo $K\alpha$) = 9·69 cm^{-1}. $R = 0{\cdot}063$ for 3255 observed reflections. The two crystallographically independent molecules are related by a pseudo inversion center. On irradiation with X-rays, the unit-cell dimensions gradually change, converging to $a = 8{\cdot}691\ (10)$, $b = 28{\cdot}05\ (2)$, $c = 8{\cdot}864\ (7)$ Å, $\beta = 114{\cdot}49\ (7)°$ and $V = 1966\ (3)$ Å^3 without degradation of crystallinity. The space group is transformed to $P2_1/a$. $R = 0{\cdot}120$ for 2452 observed reflections. One of the two cyanoethyl groups in the crystallographically independent molecules changes its configuration from *R* to *S*. The volume of the cavity for the reactive cyanoethyl group (12·61 Å^3) is greater than that for the non-reactive group (11·05 Å^3). The rate constant of the racemization, $0{\cdot}57 \times 10^{-6}$ s^{-1}, is smaller than those for related crystals, although the cavity for the reactive group is larger than the corresponding ones of those crystals. This is due to the smaller contribution of the non-reactive group to the inversion of the reactive group through the cooperative motion in the racemization process.

Introduction

It has been found that the modes of racemization of the chiral 1-cyanoethyl group in crystals of bis(dimethylglyoximato)cobalt, cobaloxime, complexes are divided into two classes: order-to-disorder and order-to-order racemization. Crystals of [(*R*)-1-cyanoethyl][(*S*)-α-methylbenzylamine]cobaloxime, *R*-cn-*S*-mba (Ohashi, Yanagi, Kurihara, Sasada & Ohgo, 1981), and [(*S*)-1-cyanoethyl][(*S*)-α-methylbenzylamine]cobaloxime, *S*-cn-*S*-mba (Ohashi, Sasada & Ohgo, 1978), reveal the first mode of racemization. Crystals of [(*R*)-1-cyanoethyl](tributylphosphine)cobaloxime, *R*-cn-tbp, and [(*R*)-1-cyanoethyl](triphenylphosphine)cobaloxime, *R*-cn-tpp, also belong to the first, although the

* To whom correspondence should be addressed.

0108-7681/84/050473-06$01.50

racemization was not observed at room temperature (Kurihara, Uchida, Ohashi, Sasada, Ohgo & Baba, 1983). The second mode is found in crystals of [(*S*)-1-cyanoethyl](pyridine)cobaloxime, *S*-cn-py (Ohashi, Yanagi, Kurihara, Sasada & Ohgo, 1982), and [(*R*)-1-cyanoethyl](4-pyridinecarbonitrile)cobaloxime, *R*-cn-cnpy (Ohashi, Uchida, Sasada & Ohgo, 1983). In both classes the racemization follows approximate first-order kinetics and the rate constant, k, was deduced from the variation of the unit cell. The cavity for the cyanoethyl group was drawn for each crystal to compare the structures around the reactive group with each other. The volume of the cavity calculated numerically has a positive correlation with the rate constant in each class, although the cavities of the first class are significantly larger than those of the second. The crystal of [(*R*)-1-cyanoethyl](4-methylpyridine)cobaloxime, *R*-cn-4mepy, was examined to clarify the further details of the racemization.

Experimental

R-cn-4mepy was prepared in a way similar to that reported previously (Ohgo, Takeuchi, Natori, Yoshimura, Ohashi & Sasada, 1981). Dark-red crystals suitable for X-ray work obtained from an aqueous methanol solution. Preliminary cell dimensions and space group deduced from photographs. Crystal $0{\cdot}30\times0{\cdot}25\times0{\cdot}15$ mm (selected carefully on a microscope) mounted on a Rigaku four-circle diffractometer. Mo $K\alpha$ radiation, graphite monochromator (45 kV, 20 mA, $\lambda = 0{\cdot}71069$ Å). Unit-cell dimensions obtained by least-squares technique with 15 reflections in the range $15° < 2\theta < 22°$. The determination of the cell dimensions was repeated continuously to register their change; this took about 30 min for each cycle. Fig. 1 shows the changes of a, b, c, β and V with the exposure time in the early stages. Intensities of $h0l$ reflections with h odd decreased significantly during the data collection and became negligibly small after 50 d (final stage). This indicates that the space group of the crystal is converted from $P2_1$ to $P2_1/a$.

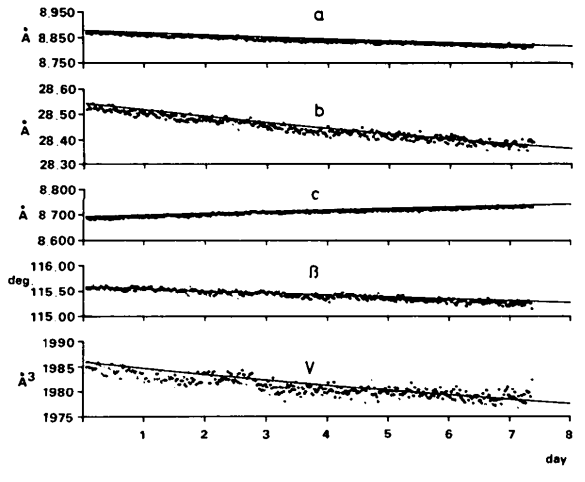

Fig. 1. Change of the unit-cell dimensions in the early stages. Solid curves represent first-order kinetics.

Three-dimensional intensity data were collected at the initial and final stages. Intensities of reflections in the range $2\theta < 50°$ for the initial stage and $2\theta < 55°$ for the final stage were measured by means of an $\omega/2\theta$ scan with a scanning rate of $8°(2\theta)\ \text{min}^{-1}$ and a scan width of $(1{\cdot}0+0{\cdot}35\tan\theta)°$. Stationary background counts were accumulated for 5 s before and after each scan. In the course of the intensity-data collection the orientation matrix was redetermined if the intensities of three monitor reflections varied significantly (greater than 8σ for the initial stage and 5σ for the final stage). Before and after the data collection at the initial stage, the unit-cell dimensions changed significantly; their average values ($a = 8{\cdot}865$, $b = 28{\cdot}505$, $c = 8{\cdot}698$ Å, and $\beta = 115{\cdot}54°$) were used throughout the structure determination.

The structure at the initial stage was solved by the direct method using the program *MULTAN*78 (Main, Hull, Lessinger, Germain, Declercq & Woolfson, 1978) and refined by the constrained least-squares method using the program *SHELX*76 (Sheldrick, 1976), to avoid parameter interaction between the two crystallographically independent molecules. In the final refinement, the non-hydrogen atoms were refined anisotropically, each bond distance was loosely constrained to have the mean value of the corresponding ones of the related compounds so far determined, and the H atoms were refined isotropically, the C–H distances being constrained to 1·00 Å. Weighting scheme: $w = [\sigma(|F_o|)^2 + 0{\cdot}0014|F_o|^2]^{-1}$. No peaks higher than 0·5 e Å^{-3} in the final difference map. Final $R = 0{\cdot}063$ for 3255 reflections.

The structure at the final stage was solved by the direct method using the program *MULTAN*78 and refined by block-diagonal least squares with the modified *HBLS* program (Ohashi, 1975). The final refinement was made with anisotropic temperature factors for the non-hydrogen atoms, isotropic for H atoms. Weighting scheme: $w = [\sigma(|F_o|) + 0{\cdot}0009|F_o|^2]^{-1}$. No peaks higher than 0·8 e Å^{-3} in the final difference map. $R = 0{\cdot}120$ for 2452 reflections. Atomic scattering factors including anomalous-dispersion terms from *International Tables for X-ray Crystallography* (1974). The atomic parameters for the non-hydrogen atoms at the initial and final stages are given in Tables 1 and 2, respectively.*

* Lists of structure factors, anisotropic thermal parameters for non-hydrogen atoms, positional and thermal parameters for H atoms and bond angles have been deposited with the British Library Lending Division as Supplementary Publication No. SUP39436 (28 pp.). Copies may be obtained through The Executive Secretary, International Union of Crystallography, 5 Abbey Square, Chester CH1 2HU, England.

Table 1. *Final atomic coordinates* ($\times 10^4$) *and equivalent isotropic thermal parameters,* B_{eq}(Å^2), *for non-hydrogen atoms at the initial stage*

$$B_{eq} = \tfrac{1}{3}\sum_i \sum_j B_{ij} a_i^* a_j^* \mathbf{a}_i . \mathbf{a}_j .$$

	x	y	z	B_{eq}
Co(*A*)	3100 (1)	3617	7762 (1)	2·7
N(1*A*)	3734 (8)	3181 (2)	9555 (8)	3·7
N(2*A*)	1404 (7)	3741 (3)	8446 (9)	3·9
N(3*A*)	2469 (9)	4045 (2)	5935 (8)	4·5
N(4*A*)	4799 (8)	3491 (3)	7076 (9)	4·1
O(1*A*)	5058 (9)	2899 (3)	9980 (11)	6·3
O(2*A*)	215 (8)	4068 (3)	7696 (13)	6·8
O(3*A*)	1142 (8)	4331 (3)	5497 (10)	6·6
O(4*A*)	6037 (9)	3185 (3)	7887 (13)	6·4
C(1*A*)	2803 (12)	3169 (4)	10361 (11)	5·3
C(2*A*)	1422 (11)	3496 (4)	9697 (11)	5·0
C(3*A*)	3424 (13)	4062 (4)	5149 (11)	6·0
C(4*A*)	4815 (13)	3740 (4)	5842 (12)	5·2
C(5*A*)	3116 (25)	2842 (7)	11791 (16)	11·4
C(6*A*)	102 (24)	3581 (8)	10277 (29)	10·3
C(7*A*)	3080 (30)	4373 (6)	3677 (14)	10·4
C(8*A*)	6096 (19)	3708 (7)	5174 (21)	9·6
N(5*A*)	4591 (7)	4118 (2)	9441 (7)	2·8
C(9*A*)	4045 (11)	4555 (3)	9435 (11)	3·9
C(10*A*)	5003 (10)	4898 (3)	10524 (11)	4·5
C(11*A*)	6599 (9)	4794 (3)	11710 (10)	3·8
C(17*A*)	7698 (16)	5160 (4)	12924 (16)	5·9
C(12*A*)	7167 (10)	4344 (3)	11748 (11)	4·4
C(13*A*)	6150 (9)	4018 (3)	10621 (10)	3·6
C(14*A*)	1640 (9)	3084 (2)	6290 (10)	3·5
C(15*A*)	2478 (14)	2687 (3)	5841 (14)	4·7
C(16*A*)	229 (11)	3258 (3)	4797 (10)	4·2
N(6*A*)	−840 (11)	3387 (4)	3590 (10)	6·1
Co(*B*)	8258 (1)	1383 (1)	7376 (2)	3·7
N(1*B*)	8926 (8)	1845 (2)	9097 (9)	4·5
N(2*B*)	6528 (7)	1313 (3)	8087 (10)	4·9
N(3*B*)	7550 (10)	924 (3)	5618 (9)	5·1
N(4*B*)	9973 (8)	1459 (3)	6661 (10)	4·5
O(1*B*)	10298 (8)	2113 (3)	9468 (11)	5·6
O(2*B*)	5311 (8)	984 (3)	7443 (12)	6·7
O(3*B*)	6192 (9)	654 (2)	5242 (11)	6·4
O(4*B*)	11184 (9)	1783 (3)	7359 (10)	5·8
C(1*B*)	8029 (11)	1894 (3)	9952 (12)	4·9
C(2*B*)	6605 (11)	1572 (3)	9350 (13)	5·7
C(3*B*)	8461 (12)	884 (3)	4780 (11)	5·4
C(4*B*)	9857 (12)	1207 (3)	5364 (11)	5·5
C(5*B*)	8407 (21)	2234 (5)	11361 (16)	7·6
C(6*B*)	5340 (19)	1576 (6)	10033 (25)	7·7
C(7*B*)	8027 (25)	527 (5)	3421 (17)	8·5
C(8*B*)	11073 (21)	1258 (6)	4635 (22)	8·3
N(5*B*)	9692 (7)	895 (2)	9114 (8)	3·5
C(9*B*)	9157 (10)	457 (3)	9128 (11)	3·9
C(10*B*)	10139 (11)	126 (3)	10274 (12)	4·3
C(11*B*)	11753 (10)	220 (3)	11448 (10)	4·0
C(17*B*)	12854 (12)	−150 (4)	12630 (14)	5·1
C(12*B*)	12261 (10)	673 (3)	11427 (11)	3·8
C(13*B*)	11247 (9)	999 (3)	10279 (10)	3·8
C(14*B*)	6977 (13)	1870 (4)	5547 (15)	7·2
C(15*B*)	7290 (27)	2379 (4)	5838 (28)	12·4
C(16*B*)	5275 (11)	1729 (4)	4517 (14)	5·7
N(6*B*)	3948 (15)	1658 (5)	3649 (20)	13·5

Table 2. *Final atomic coordinates* ($\times 10^5$ *for* Co; $\times 10^4$ *for* C, N *and* O) *and equivalent isotropic thermal parameters,* B_{eq}(Å^2), *at the final stage*

	x	y	z	B_{eq}
Co	57014 (15)	14006 (4)	75796 (15)	2·4
N(1)	6400 (9)	1856 (3)	9306 (9)	3·2
N(2)	4019 (9)	1304 (3)	8330 (9)	3·4
N(3)	4973 (9)	951 (3)	5819 (9)	3·6
N(4)	7411 (9)	1496 (3)	6797 (10)	3·5
O(1)	7778 (8)	2131 (2)	9626 (9)	4·6
O(2)	2768 (8)	974 (3)	7664 (10)	5·1
O(3)	3631 (8)	671 (2)	5488 (9)	4·9
O(4)	8667 (8)	1807 (3)	7510 (9)	4·7
C(1)	5491 (12)	1885 (4)	10157 (11)	4·0
C(2)	4058 (12)	1558 (4)	9574 (12)	3·6
C(3)	5891 (13)	925 (4)	5000 (12)	4·2
C(4)	7336 (13)	1230 (4)	5558 (12)	4·2
C(5)	5940 (17)	2218 (5)	11536 (15)	7·2
C(6)	2827 (16)	1536 (5)	10314 (17)	6·7
C(7)	5543 (19)	582 (5)	3612 (16)	7·5
C(8)	8603 (17)	1267 (5)	4867 (16)	6·8
N(5)	7169 (8)	893 (3)	9224 (8)	2·6
C(9)	6620 (11)	449 (3)	9234 (11)	3·3
C(10)	7555 (12)	111 (4)	10323 (13)	4·0
C(11)	9141 (11)	217 (3)	11503 (11)	3·0
C(17)	10223 (14)	−143 (4)	12759 (14)	4·8
C(12)	9718 (11)	676 (4)	11529 (11)	3·3
C(13)	8710 (11)	1005 (3)	10392 (11)	3·2
C(14)	4243 (11)	1937 (3)	6122 (11)	3·3
C(15)	5119 (14)	2340 (4)	5690 (13)	4·9
C(16)	2823 (12)	1750 (3)	4676 (11)	3·4
N(6)	1731 (12)	1624 (3)	3537 (11)	5·7

Results and discussion

Crystal structure

The crystal structures viewed along the *c* axis at the initial and final stages are shown in Fig. 2. The crystal at the initial stage contains two crystallographically independent molecules, *A* and *B*, which are approximately related by an inversion center except for the chiral cyanoethyl groups. When the crystal is exposed to X-rays, the cyanoethyl group of *B* is converted from the *R* configuration to *S*. The *A* cyanoethyl group, on the other hand, keeps its configuration unchanged. The pseudo inversion center then becomes a crystallographic one. This indicates that an ordered enantiomeric structure is transformed to an ordered racemic one. Such an order-to-order racemization is essentially the same as those found in the crystals of *S*-cn-py and *R*-cn-cnpy. However, the inversion center emerges between the 4-methylpyridine ligands of *A* and *B* molecules and the cyanoethyl groups contact along the glide plane in the present crystal, whereas the inversion center appears between the two independent cyanoethyl groups in the crystals of *S*-cn-py and *R*-cn-cnpy.

Molecular structure

Bond distances at the initial and final stages are given in Table 3. They are not significantly different from the corresponding ones of the related compounds. The conformation around the Co–C and Co–N bonds varies significantly before and after the racemization. The torsional angles C(16)–C(14)–Co–N(3) and N(3)–Co–N(5)–C(9) are −25·7 (7) (*A*) and 51·9 (9)° (*B*), and 46·3 (7) (*A*) and −41·3 (7)° (*B*), respectively. They become 22·8 (8)° and 42·7 (8)° at the final stage.

Reaction cavity

Fig. 3 shows stereoscopic drawings of the cavities for the cyanoethyl groups as defined in a previous paper (Ohashi, Uchida, Sasada & Ohgo, 1983). The cavity of *A* is significantly smaller than that of *B*; the volumes of the *A* and *B* cavities were calculated to be 11·05 and 12·61 Å^3, respectively. In order to compare the shapes of the two cavities, we depicted the

difference cavity by subtracting the cavity of *A* from that of *B*, after superposing the cobaloxime moieties *A* and *B*. Figs. 4(*a*) and 4(*b*) show the positive and negative regions of the difference cavity, respectively. There are rather large positive areas in the neighborhood of the cyano and methyl groups, which are just the places that can accommodate the cyanoethyl group with opposite configuration. This is probably why only the *B* cyanoethyl group can be inverted by X-ray exposure.

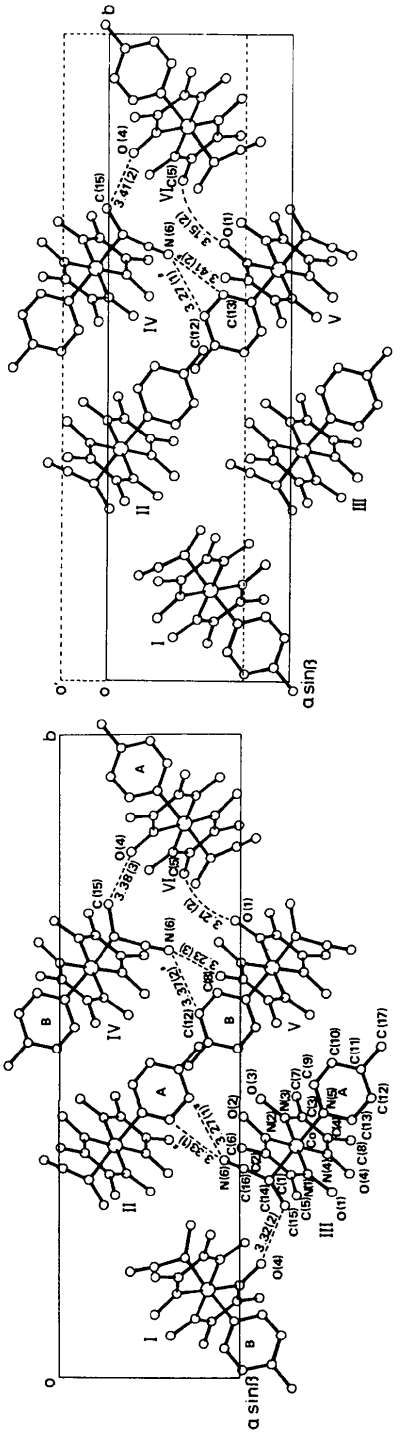

Fig. 2. Crystal structures viewed along the *c* axis (*a*) at the initial stage, and (*b*) at the final stage. The interatomic distances less than 3·4 Å are shown. The contacts between N(6*A*) and C(6*A*) in (*a*) and between N(6) and C(6) in (*b*) along the *c* axis are 3·37 (3) and 3·38 (2) Å, respectively. The dotted lines and *O'* in (*b*) indicate the unit cell and origin of the initial structure.

Fig. 5 shows the cavity for the cyanoethyl group with the *R* configuration in the final racemic structure. The shape of the cavity is similar to that of *A* in the initial structure. The volume of the final cavity, 10·27 Å^3, is smaller than those of the *A* and *B* cavities, in accordance with the contraction of the unit cell after the racemization. Fig. 6 shows the difference cavity which is obtained by subtracting the *B* cavity from the final one with the *S* configuration. The positive region, which is necessary for the inversion of the *B* cyanoethyl group, is very narrow, and the negative region, which is used for the closer packing after the racemization, is wide. This suggests that the inversion of *B* is energetically favorable.

Effect of the cooperative motion on the reaction rate

The variation of the unit-cell dimensions shown in Fig. 1 clearly indicates that the racemization follows first-order kinetics. The rate constants k_a, k_b, k_c, k_β and k_V were calculated to be $0{\cdot}53\times10^{-6}$, $0{\cdot}62\times10^{-6}$, $0{\cdot}47\times10^{-6}$, $0{\cdot}50\times10^{-6}$ and $0{\cdot}74\times10^{-6}$ s^{-1}, respectively. The average value, $0{\cdot}57\times10^{-6}$ s^{-1}, is smaller than those of *S*-cn-py and *R*-cn-cnpy. Table 4 lists the volumes of the cavities and the reaction rates

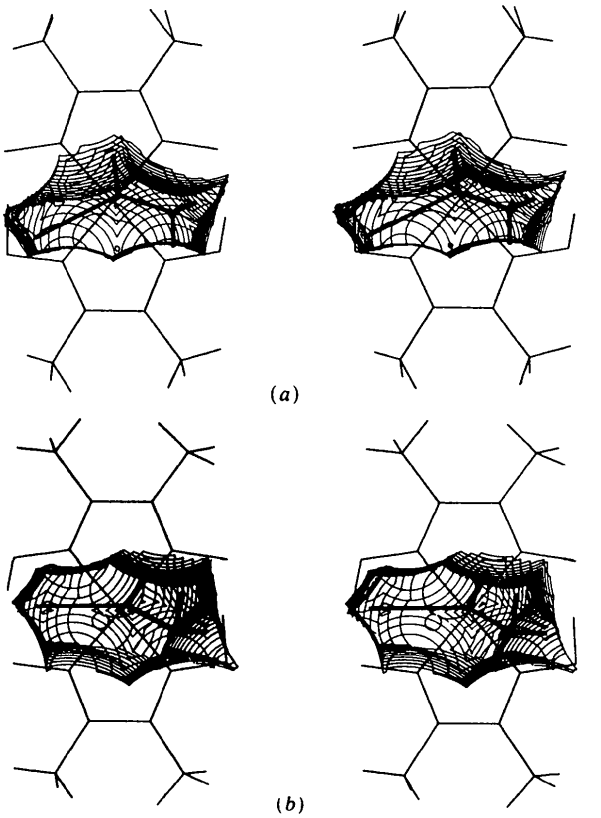

Fig. 3. Stereoscopic drawing of the cavities for (*a*) the *A* cyanoethyl group and (*b*) the *B* cyanoethyl group. Contours are drawn in sections separated by 0·1 Å.

found in the related crystals so far determined. In the crystals belonging to the second class, the cavities for the reactive *B* cyanoethyl groups are larger than those for the non-reactive *A*. However, the reaction rate of the present crystal is the smallest among the three crystals despite the cavity for *B* being the largest. In the crystals of *S*-cn-py and *R*-cn-cnpy, the *A* and *B* cyanoethyl groups face each other around the pseudo inversion center, so that their cavities are coupled together. When the *B* cyanoethyl group takes the opposite configuration, its movement could use part of the cavity for *A*; the two groups

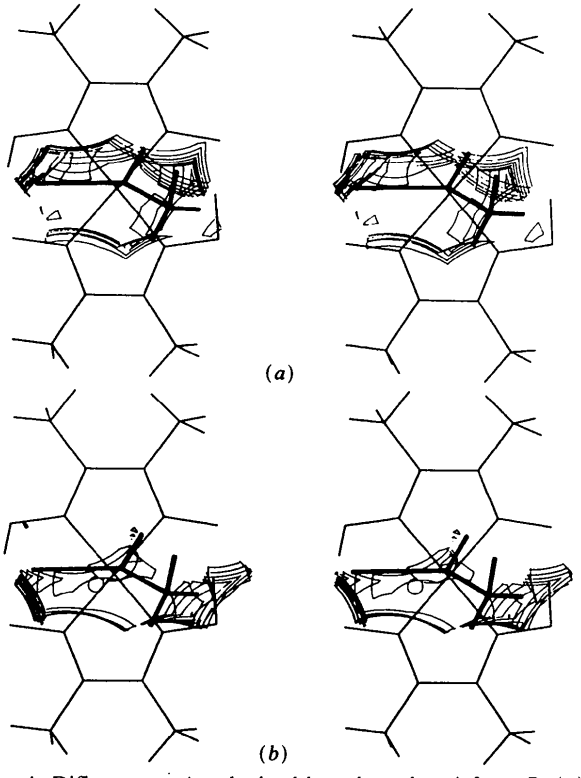

Fig. 4. Difference cavity obtained by subtracting *A* from *B*: (*a*) positive and (*b*) negative regions. Contours are drawn in sections separated by 0·1 Å.

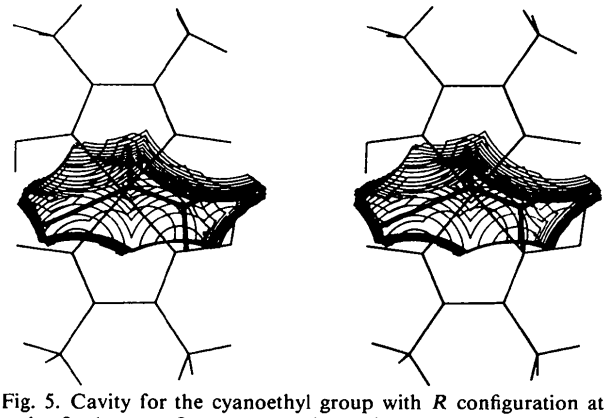

Fig. 5. Cavity for the cyanoethyl group with *R* configuration at the final stage. Contours are drawn in sections separated by 0·1 Å.

Table 3. *Bond distances* (Å) *at the initial and final stages*

	Initial (*A*)	Initial (*B*)	Final
Co–N(1)	1·879 (7)	1·887 (8)	1·890 (8)
Co–N(2)	1·873 (8)	1·895 (9)	1·860 (8)
Co–N(3)	1·887 (8)	1·903 (9)	1·899 (8)
Co–N(4)	1·878 (8)	1·888 (8)	1·901 (9)
Co–N(5)	2·064 (7)	2·045 (7)	2·058 (8)
Co–C(14)	2·05 (1)	2·05 (1)	2·05 (1)
N(1)–O(1)	1·34 (1)	1·35 (1)	1·35 (1)
N(1)–C(1)	1·29 (1)	1·31 (1)	1·30 (1)
N(2)–O(2)	1·35 (1)	1·36 (1)	1·36 (1)
N(2)–C(2)	1·29 (1)	1·30 (2)	1·30 (1)
N(3)–O(3)	1·34 (1)	1·35 (1)	1·34 (1)
N(3)–C(3)	1·30 (1)	1·31 (1)	1·28 (1)
N(4)–O(4)	1·34 (1)	1·35 (1)	1·34 (1)
N(4)–C(4)	1·29 (1)	1·30 (1)	1·31 (1)
C(1)–C(2)	1·45 (1)	1·46 (2)	1·46 (2)
C(1)–C(5)	1·48 (3)	1·48 (2)	1·46 (2)
C(2)–C(6)	1·48 (3)	1·48 (3)	1·47 (2)
C(3)–C(4)	1·44 (2)	1·45 (2)	1·43 (2)
C(3)–C(7)	1·48 (3)	1·48 (2)	1·49 (2)
C(4)–C(8)	1·49 (2)	1·48 (2)	1·47 (2)
N(5)–C(9)	1·34 (1)	1·34 (1)	1·34 (1)
N(5)–C(13)	1·35 (1)	1·35 (1)	1·35 (1)
C(9)–C(10)	1·37 (1)	1·38 (1)	1·36 (2)
C(10)–C(11)	1·38 (1)	1·38 (1)	1·37 (2)
C(11)–C(17)	1·50 (2)	1·50 (2)	1·51 (2)
C(11)–C(12)	1·37 (1)	1·37 (1)	1·38 (1)
C(12)–C(13)	1·37 (1)	1·38 (1)	1·38 (1)
C(14)–C(15)	1·49 (2)	1·48 (3)	1·50 (2)
C(14)–C(16)	1·45 (1)	1·44 (2)	1·46 (1)
C(16)–N(6)	1·13 (1)	1·11 (2)	1·12 (2)

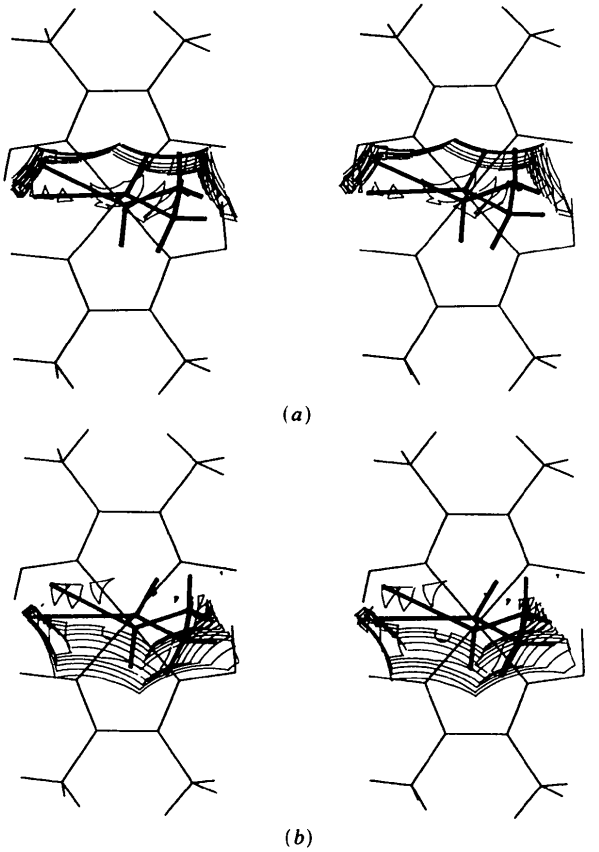

Fig. 6. Difference cavity obtained by subtracting the *B* cavity from the final one: (*a*) positive and (*b*) negative regions. Contours are drawn in sections separated by 0·1 Å.

Table 4. *Relationship between the volume of the cavity* (Å^3) *and the reaction rate k* (s^{-1})

	Volume		$k(\times 10^6)$
Class I			
R-cn-*S*-mba	14·53		3·06
S-cn-*S*-mba	12·23		2·10
R-cn-tpp	11·31		—
R-cn-tbp	10·64		—
Class II			
	(*A*)	(*B*)	
S-cn-py	8·89	11·34	2·83
R-cn-cnpy	7·97	10·37	1·65
R-cn-4mepy	11·05	12·61	0·57

around a pseudo inversion center should move cooperatively to form a racemic crystal as observed in the crystal of [(*R*)-1-methoxycarbonylethyl]-(4-chloropyridine)cobaloxime, *R*-mce-Clpy (Kurihara, Ohashi, Sasada & Ohgo, 1983). In the present crystal, on the other hand, the *A* and *B* cyanoethyl groups contact along the *a*-glide plane. The cavities for the two groups are linked infinitely along the *a* axis as shown in Fig. 7. The joining regions between the two groups in the cavity are very narrow. The cooperative motion of the two groups in the racemization process would be less than those in the crystals of *S*-cn-py and *R*-cn-cnpy. In the crystals of the first class, an ordered cyanoethyl group, isolated from the other groups, is converted to the disordered racemates, so that the larger cavity would be necessary as shown in Table 4. The above results suggest that the cooperative motion, as well as the size of the cavity, plays an important role in determining the reaction rate.

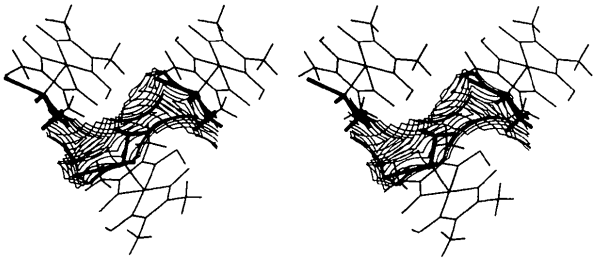

Fig. 7. Infinitely linked cavity along the *a* axis. Contours are drawn in sections separated by 0·1 Å.

This work was partly supported by a Grant-in-Aid for Scientific Research from the Ministry of Education, Science and Culture, Japan (56430005), and Itoh Science Foundation.

References

International Tables for X-ray Crystallography (1974). Vol. IV, pp. 71–151. Birmingham: Kynoch Press.

KURIHARA, T., OHASHI, Y., SASADA, Y. & OHGO, Y. (1983). *Acta Cryst.* B**39**, 243–250.

KURIHARA, T., UCHIDA, A., OHASHI, Y., SASADA, Y., OHGO, Y. & BABA, S. (1983). *Acta Cryst.* B**39**, 431–437.

MAIN, P. HULL, S. E., LESSINGER, L., GERMAIN, G., DECLERCQ, J.-P. & WOOLFSON, M. M. (1978). *MULTAN*78. *A System of Computer Programs for the Automatic Solution of Crystal Structures from X-ray Diffraction Data.* Univs. of York, England, and Louvain, Belgium.

OHASHI, Y. (1975). Unpublished version of an original program by T. ASHIDA.

OHASHI, Y., SASADA, Y. & OHGO, Y. (1978). *Chem. Lett.* pp. 743–746.

OHASHI, Y., UCHIDA, A., SASADA, Y. & OHGO, Y. (1983). *Acta Cryst.* B**39**, 54–61.

OHASHI, Y., YANAGI, K., KURIHARA, T., SASADA, Y. & OHGO, Y. (1981). *J. Am. Chem. Soc.* **103**, 5805–5812.

OHASHI, Y., YANAGI, K., KURIHARA, T., SASADA, Y. & OHGO, Y. (1982). *J. Am. Chem. Soc.* **104**, 6353–6359.

OHGO, Y., TAKEUCHI, S., NATORI, Y., YOSHIMURA, J., OHASHI, Y. & SASADA, Y. (1981). *Bull. Chem. Soc. Jpn*, **54**, 3095–3099.

SHELDRICK, G. M. (1976). *SHELX*76. Program for crystal structure determination. Univ. of Cambridge, England.

Acta Cryst. (1984), B**40**, 478–483

Crystalline-State Reaction of Cobaloxime Complexes by X-ray Exposure. X. Structural Requirement for the Racemization of the 1-Methoxycarbonylethyl Group

BY TOSHIHARU KURIHARA, AKIRA UCHIDA, YUJI OHASHI* AND YOSHIO SASADA

Laboratory of Chemistry for Natural Products, Tokyo Institute of Technology, Nagatsuta 4259, *Midori-ku, Yokohama* 227, *Japan*

(*Received* 21 *March* 1984; *accepted* 14 *June* 1984)

Abstract

Two crystalline forms of bis(dimethylglyoximato)-[(*S*)-1-methoxycarbonylethyl][(*R*)-α-methylbenzylamine]cobalt(III) (dimethylglyoximato is 2,3-butanedione dioximato), $C_{20}H_{32}CoN_5O_6$, [Co-$(C_4H_7O_2)(C_4H_7N_2O_2)_2(C_8H_{11}N)$], were obtained from an aqueous methanol solution and their structures were determined by X-ray analysis. Form (I): $M_r = 497{\cdot}4$, triclinic, $P1$, $a = 8{\cdot}637\ (1)$, $b = 8{\cdot}955\ (2)$, $c = 8{\cdot}094\ (1)$ Å, $\alpha = 105{\cdot}71\ (1)$, $\beta = 100{\cdot}18\ (2)$, $\gamma = 96{\cdot}23\ (2)°$, $V = 585{\cdot}0\ (2)$ Å^3, $F(000) = 262$, $D_x = 1{\cdot}412$ g cm^{-3}, $Z = 1$, μ(Mo $K\alpha$) = 8·11 cm^{-1}. Form (II): monoclinic, $P2_1$, $a = 8{\cdot}017\ (3)$, $b = 16{\cdot}715\ (6)$, $c = 8{\cdot}972\ (3)$ Å, $\beta = 101{\cdot}88\ (3)°$, $V = 1176{\cdot}5(7)$ Å^3,

* To whom correspondence should be addressed.

0108-7681/84/050478-06$01.50